Evolution of the Inflated Calyx Syndrome in Solanaceae

Jin-Yong Hu and Heinz Saedler

Department of Molecular Plant Genetics, Max-Planck-Institute for Plant Breeding Research, Cologne, Germany

Species that express the inflated calyx syndrome (ICS) are found in several genera of the Solanaceae. The MADS-box protein MPF2, together with the plant hormones cytokinin and gibberellin, has been shown to be responsible for this trait in *Physalis floridana*. We have used sequence data from 114 species belonging to 35 genera to construct a molecular phylogeny of Solanaceae. Apart from the 2 *Witheringia* species analyzed, species within a given genus cluster together on the resulting cladogram. *Witheringia solanacea* is embedded within the Physalinae, but *Witheringia coccoloboides* is placed basal to the Iochrominae. The ICS trait seems to be of multiple origins both within the Solanaceae and the Physaleae. Surprisingly, expression of *MPF2*-like genes in floral organs appears to be plesiomorphic in both the Physaleae and the Capsiceae. Some species in these tribes that show neither ICS nor calyx accrescence fail to express the *MPF2*-like gene in floral organs. Among those that do express this gene in the calyx are the species *Capsicum baccatum*, *Lycianthes biflora*, *Tubocapsicum anomalum*, *W. solanacea*, and *Vassobia breviflora*, all of which form small calyces that do not respond to externally applied hormones. The plesiomorphic nature of *MPF2*-like gene expression in the calyx of the Physaleae and Capsiceae raises the possibility that originally ICS also was actually a plesiomorphic character in these 2 groups. However, this trait might have undergone changes in a number of species due to secondary loss of components in ICS formation, like hormone response of calyx development. These findings are discussed in an evolutionary context of a molecular pathway leading to ICS.

Introduction

The origin of morphological novelties is a long-standing problem in evolutionary biology. The Solanaceae exhibit a remarkable diversity of floral and fruit traits, which has been extensively studied (Knapp 2002; Knapp et al. 2004). The floral architectures of *Solanum tuberosum* and *Physalis floridana* differ markedly (He and Saedler 2005). The differences in architecture become apparent following pollination/fertilization. Whereas the calyx of the *S. tuberosum* flower remains small during fruit development, the calyx of *Physalis* resumes growth and ultimately encapsulates the mature berry. The resulting structure is commonly called the "Chinese lantern" or "inflated calyx syndrome" (ICS) (He et al. 2004). The ICS has arisen several times within the Solanaceae and is a suitable model for studying the evolution of a morphological innovation. Recruitment of MPF2, a MADS-box transcription factor, from the vegetative into the floral program has been shown to be essential for the development of ICS in *Physalis*, although pollination/fertilization is also required (He and Saedler 2005). Recent work has demonstrated that treatment of cells with cytokinin facilitates the transport of MPF2 into the calyx cell nucleus, where it promotes cell division, whereas gibberellin-mediated cell elongation has been implicated in the enlargement of the calyx (He and Saedler 2007). If these 3 factors are sufficient to induce ICS, then provision of all 3 components in the calyx cells of a species that does not normally show ICS, such as potato, should cause a Chinese lantern to form. Indeed, transgenic *S. tuberosum* that ectopically express *STMADS16*, the ortholog of *MPF2*, in the calyx develop an ICS-like structure if treated with the above-mentioned plant hormones (He and Saedler 2007). ICS formation thus seems to be a multifactorial trait. However, cytokinin and gibberellin are synthesized as a consequence of pollination/fertilization, so provision of MPF2 in the calyx would seem to be the limiting step in ICS evolution (He and Saedler 2007).

At least 9 of the 96 genera in the family Solanaceae (D'Arcy 1991) display ICS. This relatively high frequency might also be compatible with a multiple origin for ICS. But alternatively, the trait could represent a plesiomorphic character that was lost in most lineages during the evolution of the Solanaceae.

In an initial attempt to decide between these possibilities, we report a molecular phylogeny of 114 solanaceous species from 35 genera, based on gene sequences including *MPF2*, which determines the development of ICS. Whereas trait analysis suggests multiple origins of ICS in the Solanaceae in general and in the Physaleae in particular, expression of *MPF2*-like genes in floral structures appears to be plesiomorphic in both the Physaleae and the Capsiceae. Additionally, other components of ICS formation–like hormone response of calyx cell proliferation and cell expansion were also analyzed. Our findings are discussed in an evolutionary context of the molecular pathway leading to ICS.

Materials and Methods

Plant Materials

A total of 262 accessions were obtained from seed banks worldwide, including 114 species representing 35 genera of Solanaceae (table 1; supplementary table 1, Supplementary Material online). All plants were grown in the greenhouse, and seeds were stored in the seed bank at the Max-Planck-Institute for Plant Breeding Research (MPIZ). Samples of young leaves and calyx material were collected separately from blooming and fruiting plants, quickly frozen in liquid nitrogen, and stored at −70 °C for nucleic acids extraction. The tiny calyces of Cap002, T001, and Wi002 plants were excised carefully using a razor blade and then processed as above.

Comparison of Calyx Morphologies

Calyx diversity was evaluated on the basis of direct measurements of calyx length and on information in published floras (D'Arcy 1973; Zhang et al. 1994). Calyx lengths were

Key words: phylogenetic analysis, *MPF2*-like, MADS-box gene, ICS, plesiomorphy, apomorphy, Physaleae, Solanaceae.

E-mail: saedler@mpiz-koeln.mpg.de.

Mol. Biol. Evol. 24(11):2443–2453. 2007
doi:10.1093/molbev/msm177
Advance Access publication September 6, 2007

Table 1
List of Taxa Used in This Study

				Calyx Architecture				
				Length (mm)[b]				
Identifier	Genus	Species	Source[a]	Flower (Fl)	Fruit (Fr)	Ratio (Fr/Fl)	Accrescence[c]	Inflation[c]
Ab001	*Atropa*	*belladonna*	BGN	13.6 ± 00.6	15.2 ± 01.8	1.12	+	−
Al001	*Anisodus*	*luridus*	BGN				−	−
Cal001	*Calibrachoa*	*parviflora*	BGN	12.1 ± 01.4	14.5 ± 01.0	1.20	+	−
Cap002	*Capsicum*	*baccatum*	BGN	01.4 ± 00.3	01.9 ± 00.4	1.37	−	−
Da002	*Datura*	*inoxia*	BGN				−	−
Du001	*Dunalia*	*fasciculata*	BGN	04.7 ± 00.3	06.6 ± 01.2	1.41	+	−
H001	*Hyoscyamus*	*aureus*	BGN	27.1 ± 01.9	28.3 ± 02.2	1.05	+	−
H002	*Hyoscyamus*	*niger*	BGN	11.0 ± 00.8	20.3 ± 03.0	1.84	+	−
I001	*Iochroma*	*australe*	BGN	07.5 ± 00.7	09.2 ± 01.6	1.22	+	−
J001	*Jaltomata*	*dentata*	BGN	03.5 ± 00.4	08.3 ± 01.0	2.40	+	−
L001	*Lycianthes*	*biflora*	BGN	05.9 ± 00.6	06.6 ± 00.8	1.12	+	−
Ly002	*Lycium*	*barbarum*	BGN	04.1 ± 00.5	03.7 ± 00.3	0.90	−	−
M001	*Margaranthus*	*solanaceus*	BGN	02.2 ± 00.2	05.8 ± 00.3	2.67	+	+
N005	*Nicandra*	*physaloides*	BGN				+	+
Ni001	*Nierembergia*	*frutescens*	BGN	10.5 ± 01.5	11.7 ± 01.5	1.12	−	−
No001	*Nolana*	*humifusa*	BGN	09.6 ± 00.7	09.8 ± 00.7	1.02	−	−
Nt002	*Normania*	*triphylla*	BGN				+	−
P004	*Physalis*	*aequata*	BGN				+	+
P007	*Physalis*	*alkekengi*	BGN				+	+
P011	*Physalis*	*alkekengi* var *alkekengi*	BGN	05.7 ± 00.3	28.3 ± 03.7	4.96	+	+
P015	*Physalis*	*angulata*	BGN	05.2 ± 00.4	29.8 ± 01.9	5.73	+	+
P018	*Physalis*	*coztomatl*	BGN	09.1 ± 00.6	24.9 ± 01.5	2.73	+	+
P022	*Physalis*	*crassifolia*	BGN				+	+
P024	*Physalis*	*curassavica*	BGN	06.0 ± 00.2	16.4 ± 01.3	2.72	+	+
P030	*Physalis*	*fuscomaculata*	BGN	07.4 ± 00.6	16.6 ± 01.7	2.23	+	+
P033	*Physalis*	*ixocarpa*	BGN	04.6 ± 00.6	22.6 ± 02.7	4.95	+	+
P035	*Physalis*	*lanceifolia*	BGN				+	+
P037	*Physalis*	*mendocina*	BGN	10.2 ± 00.5	21.6 ± 01.1	2.11	+	+
P038	*Physalis*	*mexicana*	BGN				+	+
P039	*Physalis*	*minima*	BGN	04.3 ± 00.4	26.2 ± 02.6	6.11	+	+
P055	*Physalis*	*philadelphica*	PGRU				+	+
P068	*Physalis*	*pruinosa*	BGN	03.4 ± 00.3	21.1± 02.1	6.28	+	+
P075	*Physalis*	*pubescens*	NCGRP				+	+
P103	*Physalis*	*viscosa*	BGN	09.7± 00.6	17.8 ± 02.0	1.84	+	+
P105	*Physalis*	*peruviana*	MPIZSB	09.1 ± 00.7	48.9 ± 03.0	5.36	+	+
P106	*Physalis*	*floridana*	MPIZSB	05.3 ± 00.5	34.5 ± 02.7	6.54	+	+
P130	*Physalis*	*nicandroides*	CATIE				+	+
Pc008	*Physochlaina*	*physaloides*	BGN				+	+
S032	*Solanum*	*tuberosum*	MPIZSB				−	−
S101	*Solanum*	*macrocarpon*	BGN				+	−
S201	*Solanum*	*sisymbriifolium*	BGN				+	−
Sal001	*Salpichroa*	*origanifolia*	BGN	03.5 ± 01.2	05.3 ± 00.9	1.52	−	−
Sc001	*Schizanthus*	*grahami*	BGN	10.4 ± 00.5	15.5 ± 02.1	1.49	−	−
Sas001	*Salpiglossis*	*sinuata*	BGN	14.1 ± 00.7	14.9 ± 00.9	1.06	−	−
T001	*Tubocapsicum*	*anomalum*	BGN	02.1 ± 00.3	02.0 ± 00.0	0.94	−	−
V001	*Vassobia*	*breviflora*	BGN	03.0 ± 00.4	03.0 ± 00.3	1.00	−	−
W002	*Withania*	*coagulans*	BGN	07.1 ± 01.0	15.6 ± 01.8	2.19	+	+
Wi001	*Witheringia*	*coccoloboides*	BGN	02.9 ± 00.3	07.4 ± 00.9	2.59	+	−
Wi002	*Witheringia*	*solanacea*	BGN	00.7 ± 00.1	00.9 ± 00.1	1.30	−	−

NOTE.—See supplementary table 1 (Supplementary Material online) for further information. The species received from institutions listed below were grown in glasshouses and fields in Cologne and verified for their ICS phenotype.

[a] Source shows seed banks providing seeds. BGN, Botanical and Experimental Garden of Radboud University, Nijmegen, Netherlands; CATIE, Centro Agronomico Tropical de Investigation y Ensenanza, Costa Rica; MPIZSB, seed bank of the MPIZ, (Department Prof. Salamini); NCGRP, National Center for Genetic Resources Preservation, USDA-ARS, United States Department of Agriculture, Agricultural Research Service; PGRU, Plant Genetic Resources Unit, USDA-ARS. Vouchers information and seeds can be obtained from each seed bank, except MPIZSB, which provides seeds upon request.

[b] Lengths of 7–10 calyces were measured using a Vernier scale, and standard deviations were determined.

[c] Accrescence was determined by visual observation of calyx expansion in fruiting calyx: +, accrescence; −, normal. Inflation means accrescent calyces (almost) completely encapsulating fruit: +, inflation (ICS); −, normal. NA, no fruit available.

measured in flowers and fruits (7–10 of each) using a Vernier scale. Calyx accrescence was defined as an increase in calyx length of 50% or more from flower to fruit stage. The definition of ICS was based on accrescence of the calyx after anthesis to such an extent that the fruit was (almost) completely enclosed.

Scanning Electron Microscopy of Calyx Cell Surfaces

Scanning electron microscopy (SEM) of buds, blooming flowers, and fruits from *Dunalia fasciculata* Du001, *Physalis alkekengi* var. *alkekengi* P011, *Tubocapsicum anomalum* T001, *Vassobia breviflora* V001, *Witheringia*

coccoloboides Wi001, *Witheringia solanacea* Wi002 (Physaleae), and as out-group *Capsicum baccatum* Cap002 and *S. tuberosum* S032 was carried out with a digital scanning microscope (DSM940, Zeiss, Oberkochen, Germany) according to He and Saedler (2005). For each species, 6 different areas of the calyces were examined at each of 7 developmental stages (fig. 5; supplementary fig. 3, Supplementary Material online). For each developmental stage, the surface areas of no less than 100 cells of zones 1, 2, and 3 (see fig. 5) from at least 2 independent calyces were quantified with ImageJ software (http://rsb.info.nih.gov/nih-image).

Hormone Treatment

Solutions containing 10-μM gibberellic acid GA3 or 10-μM 6-benzylaminopurine 6-BAP or both together were applied with sterile Q-tips to calyces of flower buds (from which styles and stigma had been removed) or flowers prior to pollination, according to He and Saedler (2007). Calyces (10–20) were then measured as described above for each species. The species treated were Cap002, Du001, I001, L001, P011, P105, P106, T001, V001, Wi001, and Wi002.

Nucleic Acids Isolation and Purification

DNA extraction was carried out using the DNeasy 96 Plant Kit (Qiagen, Hilden, Germany) or according to the method of Zhang and Stewart (2000). RNA contamination in these DNA samples was removed by treatment with DNase-free RNase (Qiagen).

RNA extraction was performed using the BioMol total RNA extraction kit. DNA contamination was removed by incubating the samples with RNase-free DNase I (Roche Diagnostics, Mannheim, Germany).

Gene Acquisition and Sequencing

Fragments of the chloroplast genes *atpB* and *matK* were amplified by polymerase chain reaction (PCR) from total DNA by PCR using *Taq* polymerase (Qiagen) and subsequently purified with the NucleoSpin Extract II kit (Macherey-Nagel, Düren, Germany). Gene-specific primers (*atpB*: 110F and 1252R; *matK*: 55F and 1112R; sequences are available on request) were designed according to GenBank accessions X61319 and AB040023 from *Nicotiana*. Amplified fragments were directly sequenced at the automatic DNA isolation and sequencing unit at the MPIZ.

Nuclear cDNA fragments of *MPF1*- and *MPF2*-like genes were obtained by reverse transcription of total leaf RNA from species listed in table 1 with ClonTech PowerScript II reverse transcriptase followed by PCR amplification using Qiagen *Taq* polymerase. Degenerate primers were derived from segments within the MADS domain (forward) and at the C-terminal end (reverse): for *MPF1*-like, forward 11F1 (GTGAGACAAAARATHCAGATHAAGAAGATHGACAAYTT) and reverse 11Cter (TAACTTGAGGCTWGTATCWGAGTC); for *MPF2*-like, forward 16F3 (GTTCTYTGTGATGCTGATGTTGCTCTYAT) and reverse 16C0 (TAACTTGAGGCTWGTATCWGAGTC). The resulting PCR solution was gel analyzed. Fragments with size of 0.6–1.0 kb were excised from gels, purified with the NucleoSpin Extract II kit (Macherey-Nagel), and cloned into the pGEM-T Easy Vector System (Promega, Madison, WI). Clones (5–10) obtained from each ligation were sequenced in both directions using T7 and SP6 sequencing primers.

Sequence Alignments

Sequences were first edited using the original sequencing trace file and assembled using AssemblyLIGN (Oxford Molecular Group Plc., Oxford, UK). To reduce random amplification errors, only the majority consensus sequence was retained. Some accessions gave more than 1 copy of *MPF1*-like (P004, P039, P030, P105, W002, and W006) or *MPF2*-like (P024, P039, P102, P105, W002, and W006) sequences. Preliminary maximum parsimony (MP) tree reconstructions did not reveal changes of genus relationships irrespective of the copy used. Therefore, we took the sequence showing highest identity to *P. floridana MPF1* or *MPF2* as the closest orthologs and kept them in the alignments for further analyses. All the sequences were first aligned using the ClustalW method in the MacVector package (Accelrys Inc., Cambridge, UK) and subsequently edited manually according to the alignment results using MUSCLE (Edgar 2004) and POA (Lee et al. 2002).

Construction of Phylogenetic Trees

Three data sets were used for final phylogenetic reconstruction: one set including all 261 accessions based on concatenation of the chloroplast *atpB* and *matK* sequences, one set combining *atpB*, *matK*, and *MPF2*-like sequences from selected species of Solanaceae (table 1) with *Ipomea batatas* (AY100753 for *atpB*, AJ429355 for *matK*, and AF346303 *IbMADS4* for *MPF2*) (Kim et al. 2002) as out-group (Olmstead et al. 2000; Savolainen et al. 2000), and a second data set concatenating *atpB*, *matK*, *MPF2*-like, and *MPF1*-like sequences from species of Physaleae with Capsiceae as out-groups.

Phylogenetic trees were constructed using MP and maximum likelihood (ML) implemented in PAUP4.0b10 (Swofford 2002) as well as Bayesian methods (Bayesian inference [BI]) implemented by MrBayes 3.1 (Ronquist and Huelsenbeck 2003). MP analyses were conducted by heuristic search with 1,000 random addition sequences using Tree Bisection–Reconnection branch swapping; MulTrees were selected, and 2 trees retained at each step. All characters were unordered and weighted equally. Gaps were treated as missing data. A strict consensus tree was finally computed for each data set with 1,000 replicates of bootstrap support search. ML runs using the best-fit models suggested by Modeltest3.7 (Posada and Crandall 1998) implying the hierarchical likelihood ratio test for evaluation (hLRT, Goldman 1993) with the same parameters as for the MP method but adding sequence with "as-is." BI was applied under best-fit models selected by MrModeltest2.2 (Nylander 2004) with the hLRT evaluation for all data sets using MrBayes 3.1 software. Four independent runs, each

of 4 chains, at least 1,000,000 generations, were performed with sampling every 100 trees. Burn-in was set to default 25% as suggested by the software. All analyses were repeated at least twice. Only bootstrap values and Bayesian posterior probability values above 50% were mapped onto the strict consensus of all the most parsimonious trees.

In order to assess whether a topology implying a single origin of ICS was statistically less likely than one implying multiple origins, we carried out the Kishino–Hasegawa (KH test, Kishino et al. 1990), Shimodaira–Hasegawa (SH test, Shimodaira and Hasegawa 2001), and the approximately unbiased test (Shimodaira 2002) in the CONSEL package (Shimodaira and Hasegawa 2001) after we calculated the sitewise log likelihood scores via PAUP4. The best-fit model used for these analyses is HKY $+ I + G$ suggested by Modeltest software. The KH and SH tests performed with PAUP4 with 1-tailed test gave similar results as in CONSEL. The tree forcing ICS featuring *Physalis*, *Margaranthus*, and *Withania* plants into a monophyletic group but excluding the *W. solanacea* and *T. anomalum* was taken as the constraint tree.

Expression Analysis of *MPF2*-Like Genes

Semiquantitative and real-time reverse transcription polymerase chain reaction (RT-PCR) was carried out to check expression patterns of *MPF2*-like genes in various solanaceous species. Gene-specific primers were specifically designed from within the K domain and C-terminal regions of *MPF2*-like genes. To confirm expression of *MPF2*-like genes in Cap002 and L001, an additional gene-specific primer pair was designed for the C-terminal region only but still spanning one intron (primer sequences available on request).

Total RNA from young leaves and calyx materials from flowers, buds, and fruits at different developmental stages were treated with DNase I (Roche Diagnostics). First-strand cDNA synthesis was carried out using ClonTech PowerScript II reverse transcriptase with 2 μg of total RNA in a 20-μl volume. Normalization was done using the constitutively expressed *18S* rRNA. Multiplex RT–PCR was carried out first for *MPF2*-like primer pairs for 16 cycles and continued for a further 15 cycles with *18S* primers added. The reactions were analyzed by agarose gel electrophoresis and documented with the Typhoon 8600 Phosphor Imager (Amersham, Sunnyvale, CA). All the fragments obtained were confirmed by resequencing.

Real-time RT–PCR was carried out using the Bio-Rad iQ 5 Real-Time PCR Detection System. Reactions were carried out in 25-μl reactions including 500 nmol/l of gene-specific primers and 1× iQ SYBR Green Supermix solution (Bio-Rad, Hercules, CA). The following program was employed: initial polymerase activation was at 95 °C for 3 min, then 50 cycles of 95 °C for 30 s, 60 °C for 30 s, 72 °C for 40 s, and a final melt curve analysis from 60 °C to 95 °C. Only primer pairs that showed at least 85% amplification efficiency were used. All experiments were repeated 3 times for each of 3 independent samples. Relative expression of the *MPF2*-like genes in the calyx compared with leaf (normalized with respect to *18S* rRNA expression) was evaluated according to the Pfaffl method (Bio-Rad).

Results

The ICS is found in at least 9 of the 96 genera that comprise the Solanaceae (D'Arcy 1991), including *Cuatreasia*, *Exodeconus*, *Margaranthus*, *Nicandra*, *Physalis*, *Physaliastrum*, *Physochlaina*, *Przewalskia*, and *Withania*. In this report, we studied 114 species from 35 genera of Solanaceae with special emphasis on Physaleae (table 1).

In the forthcoming sections, we will describe the calyx architecture in several species, phylogenetic analyses of markers and the trait-determining *MPF2*-like genes, expression of *MPF2*-like genes in floral organs, and calyx and cellular growth responses to hormones.

Calyx Architecture

Two basic types of calyx architecture are found in Solanaceae, characterized either by distinctly separated sepals or by partially or completely fused sepals (supplementary fig. 1, Supplementary Material online). Fusion of sepals along their entire length often yields tubular structures, as in *Datura* or *Brugmansia* (data not shown). During fruit development, calyces can change in size and/or architecture (supplementary fig. 1, Supplementary Material online).

The lengths of flower and fruit calyces were measured in various solanaceous species in order to quantify enlargement of the calyx during fruit maturation (accrescence), and the data were compared with reports from the literature (D'Arcy 1973; Zhang et al. 1994) including the visual impressions of calyx architecture described (table 1). Accrescent calyces are seen in various species of many genera, including *Hyoscyamus niger* (H002), *Jaltomata dentata* (J001), *Solanum amatopense* (S040), and *W. coccoloboides* (Wi001). ICS is found in *Margaranthus*, *Nicandra*, *Physalis*, *Physochlaina*, and *Withania*. Because 3 of these genera belong to the Physaleae, this tribe will be the main focus of our study.

Physaleae includes genera and species with diverse calyx architectures. Whereas *Margaranthus*, *Physalis*, and *Withania* all feature inflated calyces (ICS) that enclose the berry, *Witheringia*, *Tubocapsicum*, *Dunalia*, *Iochroma*, and *Vassobia* do not. *Dunalia* and *Iochroma* show slightly accrescent calyces, whereas *Vassobia* has small sepals. *Tubocapsicum anomalum* and *W. solanacea* have only rudimentary calyces, whereas *W. coccoloboides* forms an accrescent calyx.

As an initial step toward deciphering the molecular basis of ICS evolution, clarification of the phylogenetic relationships between species of the Solanaceae seems mandatory.

Phylogenetic Analyses of the Solanaceae

A strict consensus MP tree based on concatenated sequences of the plastid genes *atpB* and *matK* was established using 262 accessions of Solanaceae comprising 114 species from 35 genera (supplementary fig. 2, Supplementary Material online).

MPF2 is a nuclear gene determining the ICS trait in *P. floridana* (He and Saedler 2005). *MPF2*-like sequences from 29 genera of Solanaceae were isolated and concatenated to *atpB* and *matK* from the corresponding genera.

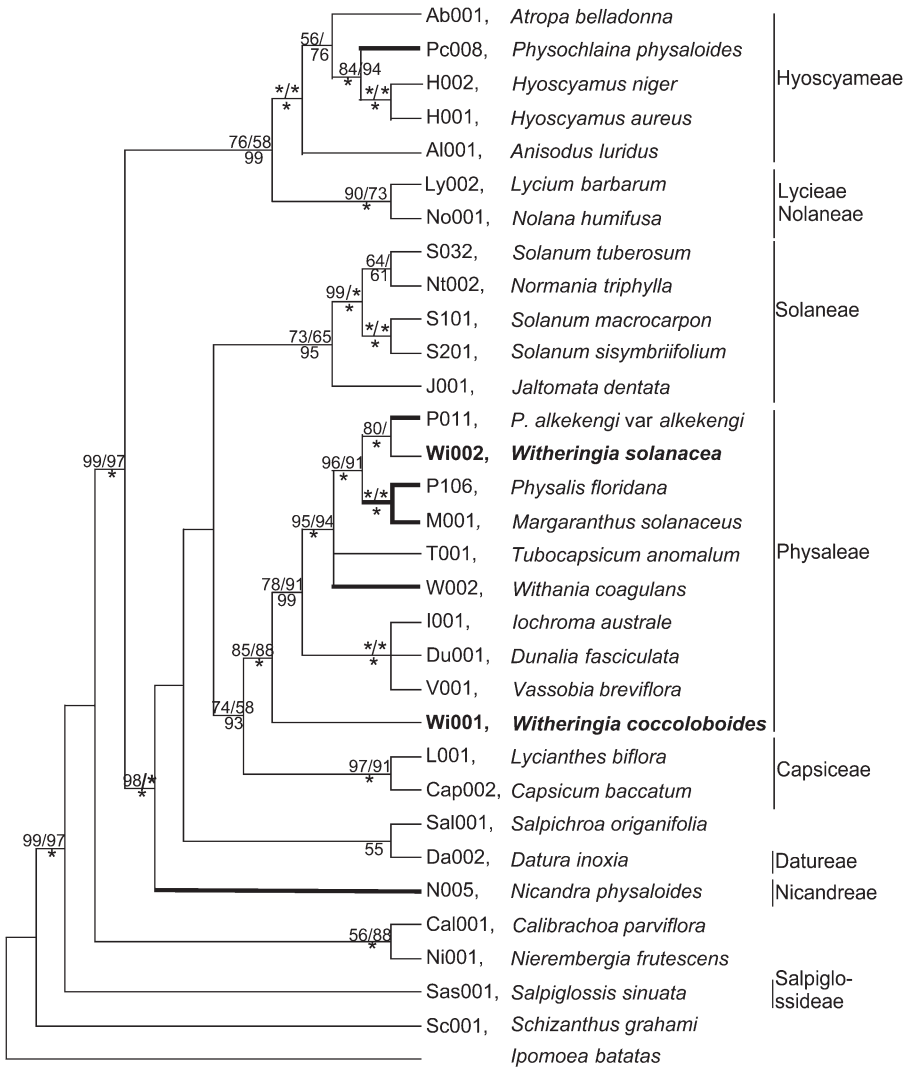

FIG. 1.—Phylogenetic analysis of Solanaceae based on concatenation of *atpB*, *matK*, and cDNA sequences of the nuclear *MPF2*-like gene. A strict consensus MP tree is given. Bootstrap values for MP (before the slash) and for ML (after the slash) are given above the branches, and Bayesian posterior probability values are shown below branches. Asterisks indicate 100% support for the branch (Material and Methods). Tree length = 1504, confidence interval = 0.6735, and retention index = 0.5756. Best-fit model used for ML analysis selected via Modeltest is TVM + *I* + *G* and for BI analysis chosen by MrModeltest is general time reversible (GTR) + *I* + *G*. Tribe classification is according to Olmstead et al. (1999). Branches in bold denote species that display ICS. The 2 nonclustering *Witheringia* species are highlighted in bold. *Ipomea batatas* was taken as out-group.

The resulting strict consensus MP tree is shown in figure 1. Its overall topology agrees well with previously published data (Olmstead and Palmer 1997; Bohs and Olmstead 1999; Olmstead et al. 1999; Gemeinholzer and Wink 2001). Interestingly, the 2 *Witheringia* species studied (fig. 1 bold) do not belong to a monophyletic group.

Branches of species featuring ICS are highlighted in figure 1 and clearly reveal multiple origins of ICS in Solanaceae.

However, establishment of multiple origins of ICS within Physaleae requires still further refinement of tree topology.

Phylogenetic Analyses of the Physaleae

MPF1 is another MADS-box transcription factor, the closest homolog of MPF2, featuring high sequence polymorphisms. MPF1 is not involved in the ICS formation (He and Saedler 2005). Unfortunately, *MPF1* is not a unique gene and therefore particular precautions had to be taken to ensure correct identification of orthology between species (see Materials and Methods).

Among the 28 species of the Physaleae tested, with *C. baccatum* and *Lycianthes biflora* as out-groups, 19 belonged to the genus *Physalis*; 2 representatives each of *Withania* and *Witheringia* were analyzed, together with one species each of *Margaranthus*, *Tubocapsicum*, *Dunalia*, *Vassobia*, and *Iochroma*. The strict consensus MP tree obtained using the 4 concatenated sequences *atpB*, *matK*, *MPF1*-like, and *MPF2*-like (fig. 2) is supported by high bootstrap and Bayesian posterior probability values. All support values are equal to or higher than 95% except among the core species of *Physalis*. Flower and fruit phenotypes for selected species are also depicted in figure 2,

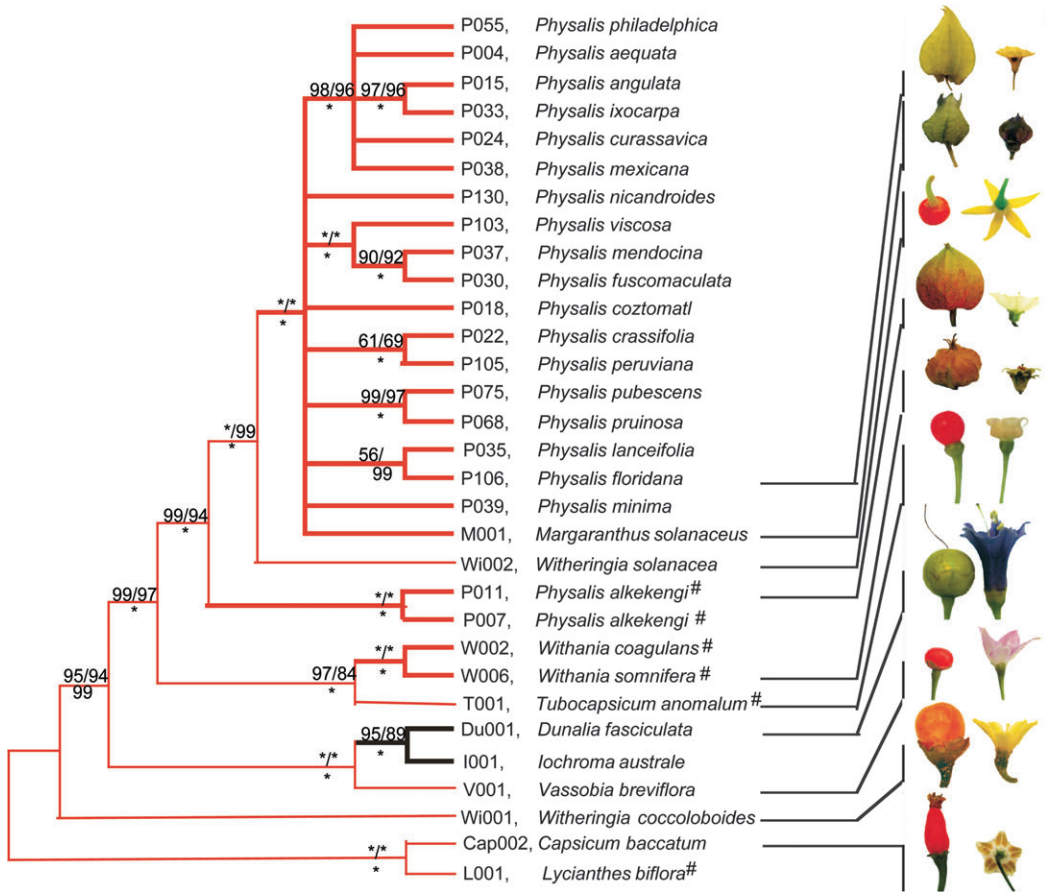

FIG. 2.—Phylogenetic tree of the Physaleae. A strict consensus MP tree with *Capsicum* and *Lycianthes* as out-groups is shown, based on concatenation of the 2 chloroplast sequences *atpB* and *matK* and cDNA sequences of the nuclear *MPF1*- and *MPF2*-like genes. Bootstrap values for 1,000 replicates for MP (first value) and ML (second value) are given above branches, and Bayesian posterior probability values are noted below branches. Asterisks indicate 100% support. Tree length = 659, confidence interval = 0.7602, retention index = 0.8013. Best-fit model used for ML analysis selected via Modeltest is HKY + *I* + *G* and for BI analysis chosen by MrModeltest is GTR + *I* + *G*. Branches leading to species that express the *MPF2*-like gene in the calyx are shown in red; bold red indicates species displaying ICS. Bold black branches denote species that show no *MPF2*-like gene expression in the calyx and do not develop ICS. The number sign (#) indicates Old World origin; all other species are of New World origin. Calyx phenotypes at flower and fruit stages are shown on the right. The vertical scale bars = 1 cm.

and the geographical origins of the species (Old World vs. the Americas) are noted. Whether or not the *MPF2*-like gene is expressed in the calyx is also indicated (see below).

Branches leading to species that develop an ICS, such as *Physalis*, *Margaranthus*, and *Withania*, are depicted as bold red lines. Note that *W. solanacea*, which does not show an ICS, is the sister taxon to the American *Physalis* species and separates the Old World *P. alkekengi* from its American relatives. *Tubocapsicum* is sister to *Withania*, which is consistent with the Old World origins of these 2 genera. The other genera and species that lack an ICS (*Dunalia*, *Iochroma*, *Vassobia*, and *W. coccoloboides*) are diverged from closer to the base of the tree. All statistical tests as described in Materials and Methods gave values of $P < 0.0001$, thus supporting the assumption of a multiple origin of ICS-bearing species within the Physaleae. This might imply that ICS itself had also arisen multiple times.

Previously, it was shown that heterotopic expression of *MPF2* in floral tissues of *P. floridana* is essential for formation of the inflated calyx (He and Saedler 2005). Therefore, species of the Physaleae that exhibit ICS should express *MPF2*-like genes in the calyx.

MPF2 Expression Studies in Various Physaleae

RNA was isolated from leaf and calyx tissues of the species indicated in figure 3 and subjected to semiquantitive RT–PCR (fig. 3*A*) and real-time RT–PCR (fig. 3*B*) using primers derived from *MPF2*-like regions (see Materials and Methods). Both techniques gave similar results.

All species that show the ICS, such as *P. floridana*, *P. alkekengi*, and *Withania coagulans*, or form an accrescent calyx, like *W. coccoloboides*, indeed express *MPF2*-like in their calyces (fig. 2 bold red lines; fig. 3). Conversely, *S. tuberosum*, *D. fasciculata*, and *Iochroma australe*, which do not develop ICS, do not express *MPF2* orthologs in their calyces (fig. 2 bold black lines; fig. 3).

However, the correlation is not absolute: *MPF2*-like RNA is found in floral tissues of a few species that do not develop ICS (fig. 2 thin red lines; fig. 3). Apart from

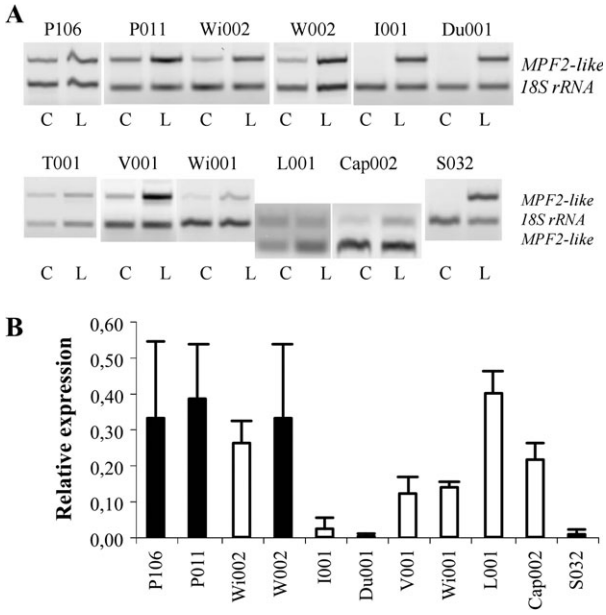

FIG. 3.—Expression of *MPF2*-like genes in the calyx. (*A*) Semi-quantitative RT–PCR analysis of *MPF2*-like expression in leaf (L) and calyx (C). Gene-specific primers used in the species shown are listed in Materials and Methods. (*B*) Real-time RT–PCR analyses with the same primer combinations as in (*A*). The black columns refer to species that exhibit ICS. The error bars indicate standard deviations (see Materials and Methods for further details). See figure 2 for species designations.

the out-groups, *C. baccatum* and *L. biflora*, these include *T. anomalum*, *V. breviflora*, and *W. solanacea*.

Surprisingly, most species tested show *MPF2*-like gene expression during floral development, implying that this represents an ancestral character. Species that express *MPF2*-like genes but do not form inflated calyces might have undergone secondary events affecting the MPF2-like protein and/or the hormone-signaling pathway. Therefore, these species were tested for their response to externally applied hormones.

Effects of Hormone Treatments on Physaleae

Treatment of ablated *P. floridana* flower buds (stigmas and styles removed to prevent fertilization) with a mixture of 6-BAP and GA_3 results in the development of ICS. The cytokinin facilitates transport of MPF2 into the nucleus, thus increasing the cell division rate. The resulting small cells enlarge upon exposure to gibberellin to form the lantern (He and Saedler 2007).

Ablated flower buds from various species of the Physaleae including *P. alkekengi* var. *alkekengi*, *Margaranthus solanaceus*, *W. solanacea*, *W. coccoloboides*, *D. fasciculata*, *I. australe*, *T. anomalum*, and *V. breviflora*, as well as *C. baccatum* and *L. biflora* for comparison, were also treated with a mixture of 6-BAP and GA_3 at early floral stages. Whereas *Physalis* and *Margaranthus* responded to the hormones by developing the ICS, none of the other species reacted, except *W. coccoloboides* (fig. 4). In this species, calyx size showed a moderate increase in size after 10 days of treatment with cytokinin alone (~20%), gibberellin alone (~30%), or both together (~35%) (fig. 4).

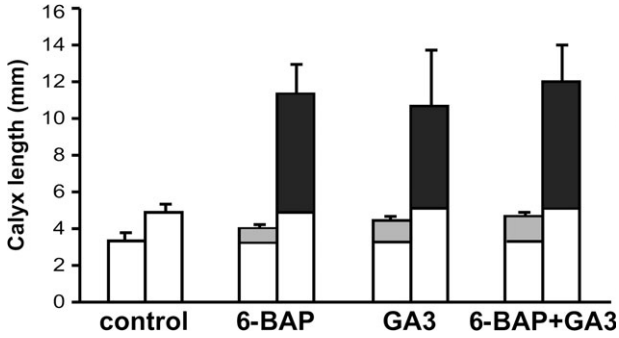

FIG. 4.—Hormone response. Flower buds of Wi001 (left column of each pair) and P106 (right column) were treated with the hormones indicated (see Materials and Methods). At least 7 calyces were measured after 10 days of treatment. The error bars indicate standard deviations. The shaded portions of the columns indicate the degree of hormone response. Note the weak effect of the hormones on Wi001.

However, calyx cell growth can vary during flower and fruit development. Calyx cell growth patterns were therefore examined more closely and quantified because this might reveal the position at which the pathway leading to ICS is blocked.

Quantification of Calyx Cell Growth

Epidermal calyx cells from various species were analyzed by SEM at different developmental stages of both flower and fruit, and their growth was quantified (fig. 5; He and Saedler 2005; supplementary fig. 3, Supplementary Material online).

Calyx cells from *P. alkekengi* (P011) were measured as representative for species with ICS (fig. 5). Cells from all zones examined (for orientation, see right picture of bottom panel in fig. 5) are small in the early stages of floral development (S1–S3). After floral egression (S4), cells of zone (1) begin to enlarge and become weakly lobate (supplementary fig. 3, Supplementary Material online; S6 and S7). By S7, zone (1) cells have increased in size more than 10-fold and are strongly lobate and elongate along the floral axis. Cells of zone (3) at the base of the calyx actually increase their surface area by up to 16-fold and are also lobate (fig. 5).

The only other species that shows lobate cells is *S. tuberosum* (S032); here, however, cell size does not increase during development (supplementary fig. 3, Supplementary Material online). All other species analyzed had nonlobate sepal cells with either square or rectangular shapes perpendicular to the floral axis (fig. 5; supplementary fig. 3, Supplementary Material online).

Vassobia breviflora exhibits a normal calyx in both flower and fruit (fig. 2). In this species, although surface areas increase about 3-fold in all zones during development, the cells remain relatively small (fig. 5).

Witheringia coccoloboides (Wi001) features a slightly accrescent calyx (fig. 5). Cell surface area is similar in all zones of the calyx but increases sharply (by ~6-fold) in the fruiting stage (S7), as in *P. alkekengi* (fig. 5, S7), though not to the same extent. During the fruiting stage (S7), cells of *W. coccoloboides* double in width along the floral axis

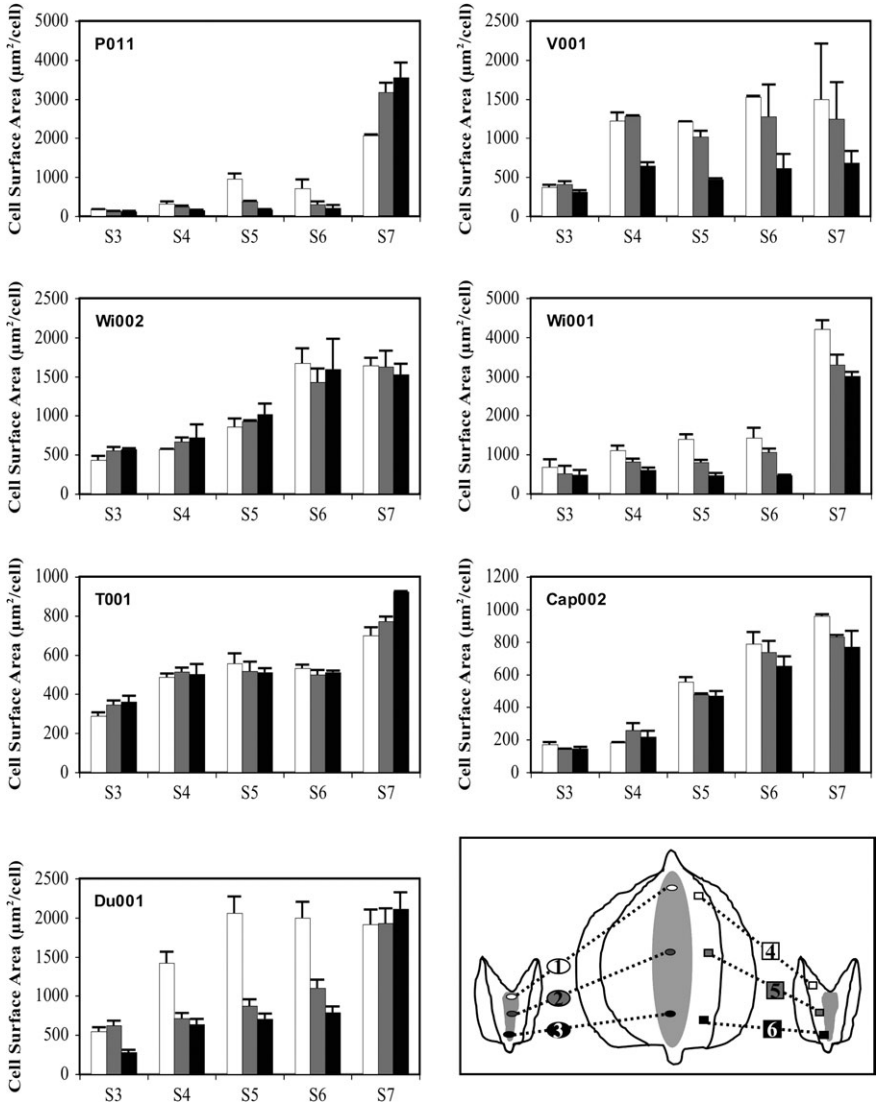

FIG. 5.—Quantification of surface areas of calyx cells at the sepal fusion region by SEM. Cell surface areas were measured in 3 zones (1, 2, and 3) of the calyx (see right picture bottom panel for orientation; results from the midrib areas 4, 5, and 6 are given in supplementary table 2, Supplementary Material online) at different stages of development (S3–S7; supplementary fig. 3, Supplementary Material online), and average cell sizes are given in square micrometers. Results are given as white (1), gray (2), and black (3) columns. At early developmental stages, S1 and S2 (supplementary fig. 3, Supplementary Material online), cell size could not be quantified due to the presence of obscuring trichomes. S3, before egression; S4, egression; S5, prior to anthesis; S6, anthesis; and S7, fruiting stage. For each zone, at least 100 cells from not less than 2 independent calyces were measured. Vertical bars indicate standard deviations. P011, *Physalis alkekengi*; Wi002, *Witheringia solanacea*; T001, *Tubocapsicum anomalum*; Du001, *Dunalia fasciculata*; V001, *Vassobia breviflora*; Wi001, *Witheringia coccoloboides*; and Cap002, *Capsicum baccatum*.

(supplementary fig. 3, Supplementary Material online; S6 and S7), which might explain the accrescence of its calyx.

Witheringia solanacea (Wi002) has a rather unremarkable small calyx and does not develop ICS. At the onset of floral development, cells are small but their surface area increases steadily in all regions of the calyx during development, becoming up to 3- to 4-fold larger in fruiting calyx. At this stage, the cell surface area was about 50% of that seen in *P. alkekengi*. Because the calyx remains very small (fig. 2), the cells apparently cease to divide during development. A similar situation was found in *T. anomalum* (T001, fig. 2). Small cells that barely increase in surface area (2- to 3-fold) during development result in an inconspicuous fruiting calyx.

In *D. fasciculata* (Du001), an increase in cell surface area is already observed in fusion zone (1) at early stages (S4 and S5) of flower development. Cells in the other zones were smaller and their surface area increased mostly in the fruiting calyx. However, the overall increase in surface area did not exceed a factor of 4, resulting in a slightly accrescent calyx.

Capsicum baccatum (Cap002) bears a small and normal calyx in flower and fruit (fig. 2). Cell surface areas in all zones increased steadily but only moderately (~4-fold).

Results for cell growth along the midrib of the sepals (supplementary table 2, Supplementary Material online; for orientation see right picture of the bottom panel in fig. 5) are similar to those reported above.

Calyces of most species tested fail to respond to hormones but those of *P. alkekengi* and *W. coccoloboides* do, although to different extents. Cells of the calyx surface in both species increase in size during development, albeit to different degrees. In *W. coccoloboides*, cell length doubles along the fruit axis, but no further cell divisions occur. This cell expansion might account for calyx accrescence in this species. In all other species, little cell surface growth is observed.

Discussion

The family Solanaceae manifests a range of biodiversity (Knapp 2002) including elaborate calyx structures such as the Chinese lantern (He et al. 2004). Thus, whereas the calyx in *S. tuberosum* remains small throughout flower and fruit development, it gets larger in *P. floridana*. In the latter, formation of the inflated calyx (ICS) requires heterotopic expression of *MPF2* during flower development, as well as exposure to the hormones cytokinin and gibberellin (He and Saedler 2005, 2007). Strikingly, *S. tuberosum* can be induced to form a lantern by appropriate manipulation: ectopic expression of *STMADS16*, the *MPF2* ortholog in *S. tuberosum*, and treatment with the above-mentioned hormones results in the formation of inflated calyces.

Therefore, ICS formation requires 3 components in the calyx: an MPF2-like protein, cytokinins, and gibberellins (He and Saedler 2007). Previously, the cytokinin 6-BAP has been shown to facilitate transport of MPF2 into the nucleus, thus promoting sepal cell division, and the resulting small cells elongate in response to gibberellins.

Given the complexity of the requirements for ICS formation, it is surprising that this trait appears to have arisen several times independently in the Solanaceae and even within the Physaleae, as suggested by our phylogenetic analyses.

Phylogenetic Relationship among the Solanaceae

The results of our phylogenetic analysis of the Solanaceae, based on concatenation of the sequences of the chloroplast marker genes *atpB* and *matK* and the nuclear *MPF2*-like sequences (fig. 1), agree well with those of previous reports (Olmstead et al. 1999; Gemeinholzer and Wink 2001; Martins and Barkman 2005).

The phylogenetic tree of the Physaleae provided here is in agreement with that of Whitson and Manos (2005), especially with respect to the positioning of *W. solanacea* and *P. alkekengi*, and also agrees with DeWitt Smith and Baum (2006) in positioning the Iochrominae within the Physaleae. However, the 2 *Witheringia* species analyzed here do not cluster together and hence should not be classified in the same genus. It has actually been suggested that these 2 species interbreed in the wild (D'Arcy 1973), but intentional crosses between them have not substantiated this (Sousa-Pena 2001). Cladistic analysis of *Witheringia* species based on morphological characters revealed no close relationship between the 2 species, but both were clearly assigned to the same genus (Sousa-Pena 2001). In our molecular phylogeny, *W. solanacea* clearly separates the Old World *P. alkekengi* from its New World relatives, whereas *W. coccoloboides* diverges earlier in the Physaleae. Clarification of the placement of *Witheringia* will require broader sampling of the taxon.

In any case, the phylogeny based on cDNA sequences of *MPF2*, the ICS-determining gene, matches the topology of the species tree as inferred from the cp data, indicating not only that the subtribes of the Solanaceae are polyphyletic but also that the ICS has arisen multiple times. Even within the Physaleae, ICS seems to have evolved several times independently.

However, the *MPF2*-like gene expression studies do not support this hypothesis but rather suggest an alternative: plesiomorphic nature of *MPF2*-like gene expression and secondary mutations in the ICS pathway.

Plesiomorphic Nature of *MPF2*-Like Gene Expression

Expression studies of *MPF2*-like genes in the calyx of different species of Physaleae yielded some surprises. All species that display ICS expressed their *MPF2*-like genes in the calyx, as expected. But some species that do not develop ICS also express the *MPF2*-like gene in their calyx. This latter category is of interest because it is compatible with the notion that expression of the *MPF2*-like gene in the calyx, although necessary, is not sufficient to induce ICS: exposure to the hormones cytokinin and gibberellin is also required (He and Saedler 2007).

On the whole, expression of *MPF2*-like genes in floral organs seems to be a plesiomorphic trait within the Physaleae and the Capsiceae. Only the heterogeneity observed in the Iochrominae challenges this inference: whereas *V. breviflora* expresses its *MPF2*-like gene in the calyx, *I. australe* and *D. fasciculata* do not (figs. 1 and 2). Note that none of the Iochrominae exhibits ICS.

Therefore, the expression of *MPF2*-like genes in the calyx of most of the Physaleae suggests that it represents a plesiomorphic character in this tribe.

The Multiple Loss versus Multiple Gain Scenario of ICS

Whereas phylogeny reconstructions suggest independent multiple origins of ICS, expression of the trait-determining *MPF2* gene in floral tissues, however, seems to be plesiomorphic. Therefore, ICS might have arisen multiple times or multiple losses might have occurred in the evolution of non-ICS featuring species. MPF2 is an essential, highly integrated component of several pathways, one leading to ICS formation (He and Saedler 2007). The likelihood of de novo appearance of ICS might depend on the predisposition of the species concerned, that is, how many components of the ICS pathway are already available. Even assuming that all but one component were present, the frequency of the gain of function of the limiting factor might still be low. In another species evolving ICS, the predisposition might not have been as optimal and hence the evolution of ICS might have been less likely. Conversely, a loss-of-function mutation is more frequent, especially if many targets are available in the pathway as in ICS formation (He and Saedler 2007, fig. 6). In this latter scenario,

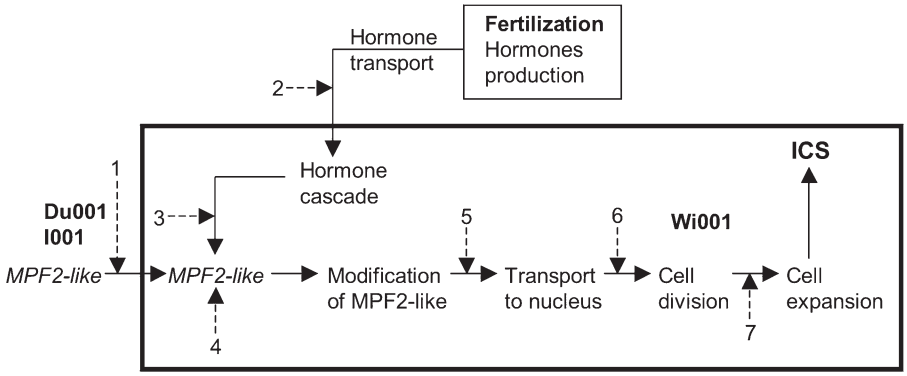

FIG. 6.—Biosynthetic pathway of ICS formation in the Physaleae. Events occurring in the calyx that lead to the ICS are depicted in the box. The numbered arrows indicate positions of possible secondary mutational events that might have occurred to interfere with ICS formation during evolutionary divergence (see text). The scheme is modified from He and Saedler (2007).

ICS represents the ancestral state and non-ICS featuring solanaceous species would be apomorphic.

Secondary Mutations Affecting the ICS Pathway

A pathway for ICS formation involving numerous steps is shown in figure 6 (modified after He and Saedler 2007). The isolation of mutants affecting these steps could permit us to better define the evolution of ICS, and a mutagenesis program in *P. floridana* is currently underway. However, wild species can be considered as "evolutionary" mutants, and hence they might also contribute to deciphering the ICS pathway. This later approach was taken here and thus allows defining already some of the steps.

Given the *MPF2*-like gene expression as a plesiomorphic character, the lack of it as in *Dunalia* and *Iochroma* provides an example of a probable secondary mutation preventing expression in the calyx (fig. 6, step 1). Therefore, *Dunalia* and *Iochroma* seem to represent derived, apomorphic states.

Step 2 affects hormone transport from the ovaries in the innermost to the outer whorl, the calyx, and very likely involves numerous functions. Mutants in long distance hormone transport might feature calyces throughout their development, which, however, upon external application of hormones might respond with secondary calyx growth. No such evolutionary mutant was found among the species tested.

Mutants in steps 3, 4, and 5, which summarize various functions in the hormone cascade, MPF2-like protein structure and modification and its nuclear transport should not respond to externally applied hormone. *Capsicum baccatum*, *L. biflora*, *T. anomalum*, *V. breviflora*, and *W. solanacea*, all express *MPF2*-like genes in floral organs, but none show ICS. They might have acquired secondary mutations in these steps because calyx growth in these species no longer responds to externally applied hormones. The simple tests applied do not allow defining these steps more precisely.

Step 6 implicates calyx cell division and step 7 deals with calyx cell elongation each along both axes, perpendicular, and along the floral axis. The accrescent calyx observed in the fruiting stage of *W. coccoloboides* seems to reveal a residual response to hormones because the cells elongate along the floral axis, very likely without further cell divisions (fig. 6, step 6).

The inconspicuous small calyx of *W. solanacea*, however, might result from interference by the MPF2-like protein with components of normal sepal cell division, or it might be the consequence of an independent defect in calyx development. Functional analysis of these MPF2-like proteins in transgenic plants might allow us to distinguish between these possibilities. Alternatively, MPF2-like proteins from different species might have different spectra of interacting proteins, which could be analyzed in yeast 2-hybrid systems.

The complexity of the mechanism underlying development of an ICS should make the process vulnerable to secondary loss-of-function mutations. Thus, it is not surprising to find so many Physaleae species that lack an inflated calyx.

Based on the comparison of *S. tuberosum* and *P. floridana* and assuming a small calyx as a plesiomorphic character, we previously suggested that ICS had evolved as a morphological novelty in response to recruitment of a vegetative transcription factor—an MPF2-like protein—into a floral program (He and Saedler 2005). Now it appears that the ICS might be the plesiomorphic trait and a small calyx the apomorphic state—at least in the Physaleae and the Capsiceae. Because most of the higher plants exhibit small calyces, one wonders whether that relationship is stable throughout the Solanaceae. Preliminary experiments (data not shown) indicate that constitutive expression of *MPF2*-like, though at different levels, is observed in most of the species listed in figure 1 (*S. tuberosum*, *I. australe*, and *Dunalia breviflora* are exceptions), indicating that within the Solanaceae constitutive expression of *MPF2* might also be plesiomorphic as well. This raises the intriguing possibility that ICS might actually be a plesiomorphic basal character in the family. Enlarged calyces including ICS are found frequently in the Solanaceae, but species lacking this trait may provide a more informative resource for the analysis of the ICS pathway.

Supplementary Material

Supplementary figures 1–3 and tables 1 and 2 are available at *Molecular Biology and Evolution* online

(http://www.oxfordjournals.org). All the sequences reported in this study have been submitted to European Molecular Biology Laboratory (EMBL) Nucleotide Sequence Database (http://www.ebi.ac.uk/embl) and GenBank (http://www.ncbi.nlm.nih.gov) under the following accession numbers: *atpB*, AM233098–AM233361; *matK*, EF438820–EF439084 and EU128753-EU128756; *MPF1*-like, EF395136–EF395173; and *MPF2*-like, EF395174–EF395229.

Acknowledgments

We thank Mrs Britta Grossardt for technical help and Dr Kerstin Hoef-Emden for the assistance in the statistical analysis. In addition, we appreciate the valuable suggestions for improving the manuscript made by Drs Chaoying He, Juliette de Meaux, Thomas Muenster, Kuert. Stueber, and Sabine Zachgo and the 2 anonymous reviewers. This work was supported by a Max-Planck-Gesellschaft Fellowship awarded to J-Y.H.

Literature Cited

Bohs L, Olmstead RG. 1999. *Solanum* phylogeny inferred from chloroplast DNA sequence data. In: Nee M, Symon DE, Lester RN, Jessop JP, editors. Solanaceae IV: advances in biology and utilization. Kew (UK): Royal Botanic Gardens. p. 97–110.

D'Arcy WG. 1991. The Solanaceae since 1976, with a review of its biogeography. In: Hawkes JG, Lester RN, Nee M, Estrada N, editors. Solanaceae III: taxonomy, chemistry, evolution. Kew (UK): Royal Botanic Gardens. p. 75–137.

DeWitt Smith S, Baum DA. 2006. Phylogenetics of the florally diverse Andean clade Iochrominae (Solanaceae). Am J Bot. 93:1140–1153.

Edgar RC. 2004. MUSCLE: multiple sequence alignment with high accuracy and high throughput. Nucleic Acids Res. 32: 792–797.

Gemeinholzer B, Wink M. 2001. Solanaceae: occurrence of secondary compounds versus molecular phylogeny. In: Berg RG, Barendse GWM, Weerden GM, Mariani C, editors. Solanaceae V: advances in taxonomy and utilization. Nijmegen University Press, Nijmengen, the Netherlands. p. 165–178.

Goldman N. 1993. Statistical tests of models of DNA substitution. J Mol Evol. 36:182–198.

He C, Münster T, Saedler H. 2004. On the origin of floral morphological novelties. FEBS Lett. 567:147–151.

He C, Saedler H. 2005. Heterotopic expression of *MPF2* is the key to the evolution of the Chinese lantern *of Physalis*, a morphological novelty in Solanaceae. Proc Natl Acad Sci USA. 102:5779–5784.

He C, Saedler H. 2007. Hormonal control of the inflated calyx syndrome, a morphological novelty, in *Physalis*. Plant J. 49:935–946.

Kim SH, Mizuno K, Fujimura T. 2002. Isolation of MADS-box genes from sweet potato (*Ipomoea batatas* (L.) Lam.) expressed specifically in vegetative tissues. Plant Cell Physiol. 43:314–322.

Kishino H, Miyata T, Hasegawa M. 1990. Maximum likelihood inference of protein phylogeny and the origin of chloroplasts. J Mol Evol. 31:151–160.

Knapp S. 2002. Tobacco to tomatoes: a phylogenetic perspective on fruit diversity in the Solanaceae. J Exp Bot. 53:2001–2022.

Knapp S, Bohs L, Nee M, Spooner DM. 2004. Solanaceae, a model for linking genomics with biodiversity. Comp Funct Genomics. 5:285–291.

Lee C, Grasso C, Sharlow MF. 2002. Multiple sequence alignment using partial order graphs. Bioinformatics. 18:452–464.

Martins TR, Barkman TJ. 2005. Reconstruction of Solanaceae phylogeny using the nuclear gene SAMT. Syst Bot. 30:435–447.

Nylander JAA. 2004. MrModelTest, 2.0th edition. Upsalla, Distributed by the author: Evolutionary Biology Centre: Uppsala University, Uppsala, Sweden.

Olmstead RG, Kim KJ, Jansen RK, Wagstaff SJ. 2000. The phylogeny of the Asteridae sensu lato based on chloroplast *ndhF* gene sequences. Mol Phylogenet Evol. 16:96–112.

Olmstead RG, Palmer JD. 1997. Implications for the phylogeny, classification, and biogeography of *Solanum* from cpDNA restriction site variation. Syst Bot. 22:19–29.

Olmstead RG, Sweere JA, Spangler RE, Bohs L, Palmer JD. 1999. Phylogeny and provisional classification of the Solanaceae based on chloroplast DNA. In: Nee M, Symon DE, Lester RN, Jessop JP, editors. Solanaceae IV: advances in biology and utilization. Kew (UK): Royal Botanic Gardens. p. 111–137.

Posada D, Crandall KA. 1998. Modeltest: testing the model of DNA substitution. Bioinformatics. 14:817–818.

Ronquist F, Huelsenbeck JP. 2003. MRBAYES 3: Bayesian phylogenetic inference under mixed models. Bioinformatics. 19:1572–1574.

Savolainen V, Chase MW, Hoot SB, Morton CM, Soltis DE, Bayer C, Fay MF, de Bruijn AY, Sullivan S, Qiu YL. 2000. Phylogenetics of flowering plants based upon a combined analysis of plastid *atpB* and *rbcL* gene sequences. Syst Biol. 49:306–362.

Shimodaira H. 2002. An approximately unbiased test of phylogenetic tree selection. Syst Biol. 51:492–508.

Shimodaira H, Hasegawa M. 2001. CONSEL: for assessing the confidence of phylogenetic tree selection. Bioinformatics. 17:1246–1247.

Sousa-Pena M. 2001. Systematics and reproductive biologoy of the genus Witheringia L'Her (Solanaceae). [PhD thesis]. (UMI number: 3008142). Bell & Howell Information and Learning Company, Ann Arbor, MI.

Swofford DL. 2002. PAUP*: phylogenetic analysis using parsimony (*and other methods). Version 4.0b10. Sunderland (MA): Sinauer Associates.

Whitson M, Manos PS. 2005. Untangling *Physalis* (Solanaceae) from the Physaloids: a two-gene phylogeny of the Physalinae. Syst Bot. 30:216–230.

Zhang Z, Lu A, D'Arcy WG. 1994. Solanaceae. In: Wu Z, Peter HR, editors. Flora of China, Vol. 17 (Verbenaceae through Solanaceae). Beijing: Science Press; St Louis: Missouri Botanical Garden Press. p. 300–332.

Zhang J, Stewart J. 2000. Economical and rapid method for extracting cotton genomic DNA. J Cotton Sci. 4:193–201.

Neelima Sinha, Associate Editor

Accepted August 16, 2007